A fluidic lens with reduced optical aberration

Jei-Yin Yiu, Robert Batchko*, Sam Robinson, Andrei Szilagyi
Holochip Corporation, 4940 W. 147th Street, Hawthorne, CA USA 90250

ABSTRACT

We present an electrically-actuated adaptive fluidic lens having a 10-mm aperture, 4-diopter range and center-thickness less than 1 mm. The lens employs dual deflectable glass membranes encasing an optical fluid. A piezoelectric ring bender actuator draws less than 1 mW and is built into the 25-mm-diameter lens housing. The adaptive lens demonstrates resolution comparable to commercial precision glass singlet lenses of similar format over a wide range of field angles and focal powers. Focal power vs. voltage, resolution, modulation transfer function (MTF), life testing and dynamic response are examined and show that the lens is suitable for numerous adaptive lens applications demanding high optical quality.

Keywords: fluidic lens, adaptive lens, liquid lens, zoom lens, adaptive optics, autofocus, piezoelectric, electroactive polymer

1. INTRODUCTION

In the continuous drive to offer consumers smaller, lighter, slimmer and more portable electronics products, fluidic (or "liquid") lenses have emerged as a promising candidate for the miniaturization of camera optics in these devices.[1] Numerous fluidic lens technologies have been researched and, to date, several have been commercialized (e.g., electrowetting[6], liquid crystal[7,8], etc.). Of these, one well-known approach, based on a flexible membrane encasing a fluid[2,3,4,5,16,17], is particularly attractive due to its manufacturability, wide range in focal power, fast response, high optical transmission, scalability in size and compatibility with numerous actuation technologies. However, due to the inherent elasticity of the membranes, these fluidic lenses generally tend to suffer from optical aberrations such as spherical aberration and gravity-induced coma. Techniques for counteracting aberrations in such membrane-delimited fluidic lenses have been explored and include the following: a) assembling the lens with the membrane fastened under tension in order to increase its stiffness[10,11]; b) disposing fluids of different refractive index but similar density on either side of the membrane to neutralize gravity-induced stress on the membrane[9]; and c) replacing the typical elastomeric membrane[13,14,15] with a material having a much larger Young's modulus such as thin glass or plastic[12]. The tensioned-membrane approach offers increased stiffness and sufficient compliance to provide a wide dioptric range, but still suffers from aberrations. The dual-fluid approach, while balancing gravity-induced stress, suffers from an increase in lens thickness, weight and response time while reducing the dioptric range. The third approach, using higher-modulus membranes, significantly reduces aberrations, but at the cost of reduced dioptric range. This paper presents a fluidic lens based on high-modulus membranes; in particular, membranes composed of thin, flexible glass. In addition to improved optical performance, the present design offers a large fill factor (i.e., the ratio of aperture diameter to external housing diameter), thin center thickness and reduced risk of leakage of the optical fluid.

*rgb@holochip.com; phone 1 650 650-1064; www.holochip.com

2. DESIGN

As shown in Figure 1, the fluidic lens[12] consists of a lens chamber made of a first 70-µm-thick glass membrane bonded to the internal surface of a precision-machined aluminum housing with an elastomeric seal. A second 70-µm-thick glass membrane is similarly bonded to a precision-machined aluminum plate. The elastomeric seals help prevent leakage of the fluid at the edge of the membrane. The seals also allow the membranes to bend over their entire surface and pivot at their edge; this enables the membranes to achieve a more spherical curvature throughout the aperture, generally improving optical performance. An elastomeric gasket seals the chamber and connects the plate to the housing while allowing the plate to move axially in the housing by several hundred µm. The lens chamber is filled with an optical fluid (e.g., n = 1.3 to 1.6). A stack of piezoelectric bending actuators is mounted inside the housing between the plate and an adjustable threaded section of the housing. The adjustable housing section can be selectively positioned in order to control the preload on the piezo stack, and, hence, the initial focal power of the lens. Application of a voltage to the piezo stack causes the stack to strain axially, thereby increasing or decreasing the pressure in the lens chamber. An increase in pressure in the lens chamber results in the glass membranes bending outward (i.e., in a convex fashion). Likewise, a decrease in pressure in the lens chamber results in the glass membranes bending inward (i.e., in a concave fashion). The outer diameter of the housing is 25.4 mm (1 inch) and includes a 1.035-40 threaded section, compatible with standard 1-inch lens mounts. The inner diameter of the piezo stack is 10 mm and defines the aperture of the lens. An optional window or static optical element may be mounted in the housing in close proximity to the membranes.

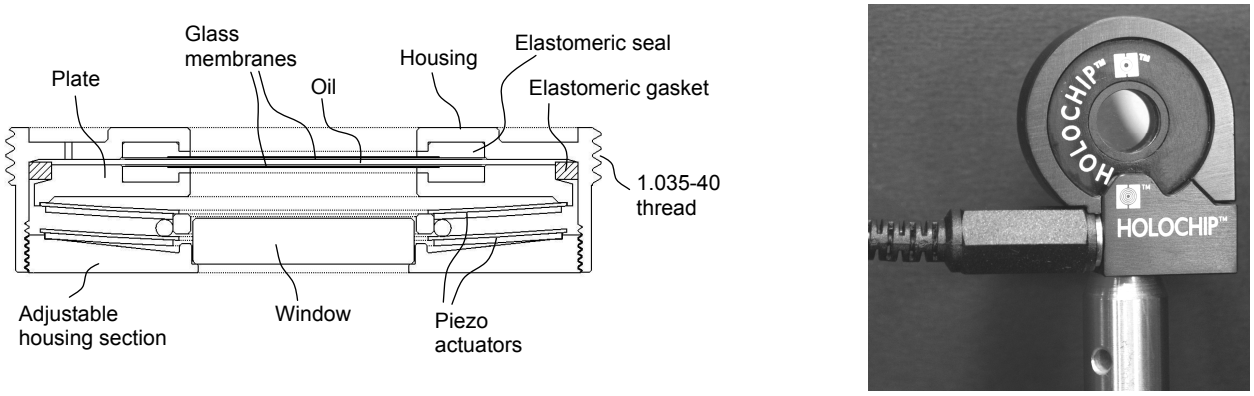

Figure 1. Fluidic lens with glass membranes: cross-section illustrated view (left); photo of lens[12] in custom 1-inch lens mount (right)

A DC-to-DC step-up converter is used to provide voltage to the piezo stack, and to allow the lens to be controlled by a convenient program voltage of 0-to-5 VDC while drawing less than 1 mW for quasi-static operation. A schematic diagram of the step-up converter is shown in Figure 2.

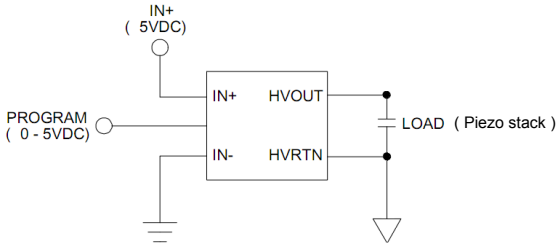

Figure 2. Schematic diagram for the DC-to-DC step-up converter

3. OPTICAL PERFORMANCE

The fluidic lenses were characterized for focal power dependence on voltage, resolution, MTF and useful lifetime.

Focal power vs. program voltage

Focal length and refractive power as functions of program voltage are plotted in Figure 3. The focal length of our fluidic lenses was determined using a collimated input light beam by measuring the location of the smallest waist along the optical axis. The same collimated white light was used as the light source during this series of measurements. Initially, no voltage was delivered to the fluidic lens. The voltage was then increased to 1 VDC and the measurement repeated. This process was repeated in 1-V increments up to 5 VDC. The voltage was then returned to 0, again by 1-VDC intervals with similar focal length measurements taken at each voltage level. The plot shows hysteresis which is common in piezoelectric actuators.[3] The focal length ranges from approximately 200 to 900 mm and the range in diopters is approximately 4 dpt.

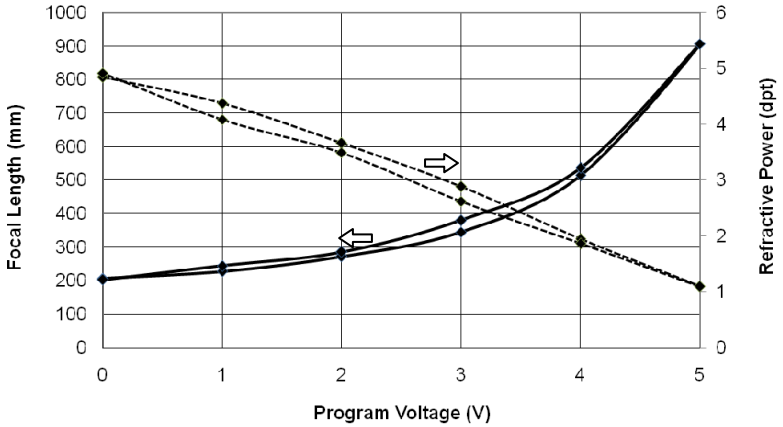

Figure 3. Focal length and refractive power vs. program voltage

1951 Air Force resolution target imaging

The imaging quality of a set of four Holochip fluidic lenses was benchmarked against 1-inch-diameter Newport Corporation precision glass lenses (Newport models KBX082 and KBX079). Both the Newport and Holochip lenses were set at approximately 250-mm and 500-mm focal lengths. Biconvex Newport lenses were selected in order to provide an optical surface geometry similar to that of the Holochip fluidic lenses. A 10-mm-diameter aperture stop was placed in close proximity to the Newport lenses in order to provide the same aperture as that of the Holochip lenses. The Holochip lenses were uncoated; the Newport lenses were visible-anti-reflection (VIS AR) coated.

The experimental set-up for imaging the resolution target is shown in Figure 4. The devices under test (DUTs) were arranged for one-to-one imaging. The object source was a 1951 USAF resolution target (Edmund Optics NT38-256), which was backlit with white light and a diffuser fashioned from slide glass and translucent tape. Images were captured on a Sony XC ST50 camera. For a given focal length of the DUT (i.e., 250 or 500 mm), the target and camera were spaced 4 focal lengths (4*f*) apart with the DUT halfway between the two. Images were captured at field angles of 0, 5, 10 and 15 degrees by rotating the DUT relative to the optical axis of the system. The optical axis of the system was oriented horizontal to the ground, thereby maximizing the potential for gravity to induce aberrations in the fluidic lenses. In order to reduce background noise in the captured images due to stray light, beams tubes composed of opaque PVC pipe were placed along the optical axis of the system.

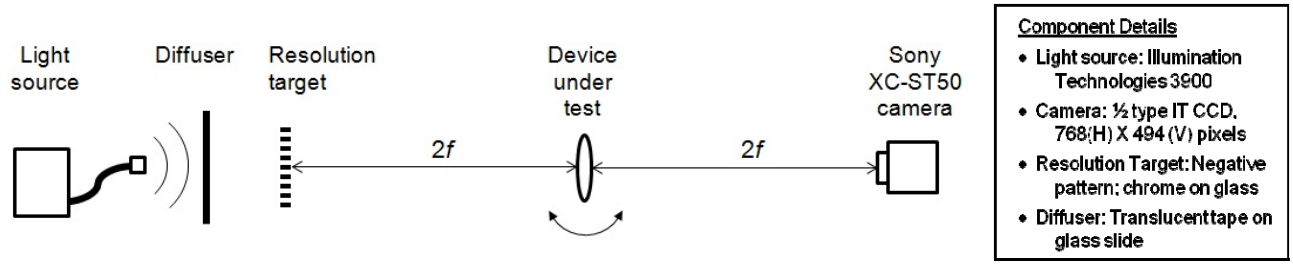

Figure 4. Experimental set-up for AF resolution target imaging

For calibrating the set-up, a Newport lens (e.g., Newport model KBX082 having a 500-mm focal length) served as a reference lens and was used to align the system. After capturing an image, a Holochip fluidic lens replaced the Newport lens and the program voltage was adjusted until the camera registered the best-focused image. Images were collected in this fashion for four Holochip lens samples. This process was then repeated with each of the DUTs rotated at 5, 10 and 15 degrees to the system optical axis. Next, a Newport model KBX079 lens, having a 250-mm focal length, was placed in the system and the AF target, camera and beam tubes were repositioned accordingly. Again, after capturing an image with the 250-mm-focal-length Newport lens, a Holochip fluidic lens replaced the Newport lens and the program voltage was adjusted for best focus. Images were again collected in this fashion for the same four Holochip lens samples as before. This process was also repeated for field angles of 5, 10 and 15 degrees.

As the best focus was determined based on a visual assessment of the captured image, some degree of error is intrinsic. A notable variation in resolution and focus is detectible by the human eye with a change in program voltage of only 0.01-VDC. Therefore, it is assumed that the voltage applied results in a focal length very near the desired value, and, hence, best-focus condition.

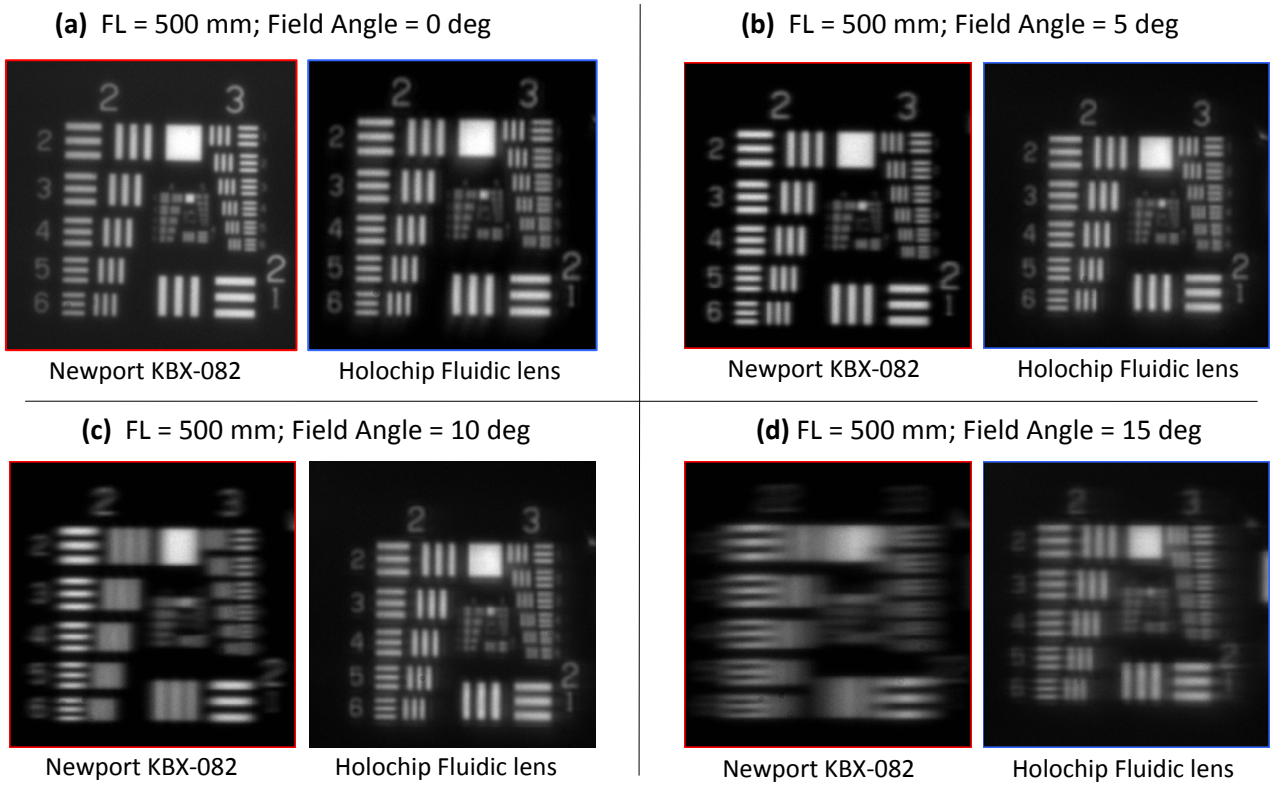

Figure 5. Air Force resolution target imaging for 500-mm-focal-length Newport and Holochip lenses at field angles of: (a) 0 deg; (b) 5 deg; (c) 10 deg; and (d) 15 deg

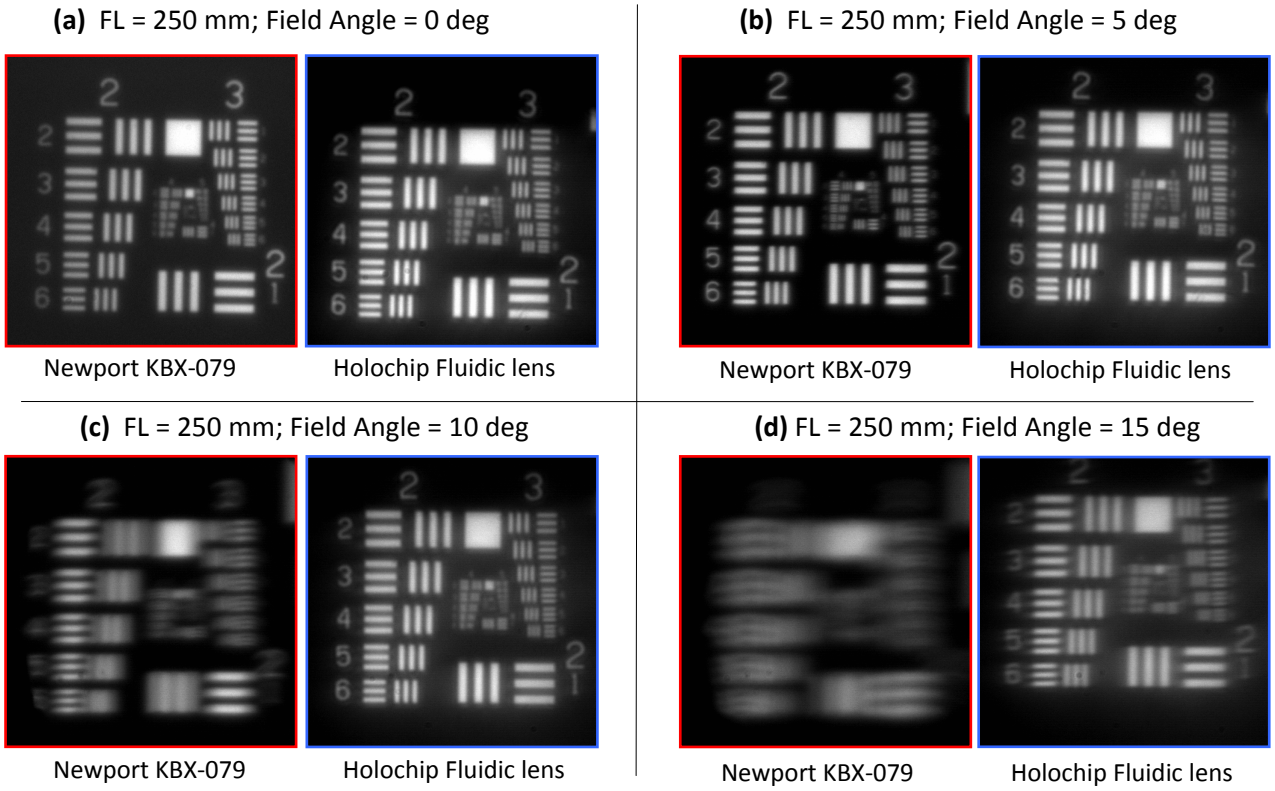

Figure 6. Air Force resolution target imaging for 250-mm-focal-length Newport and Holochip lenses at field angles of: (a) 0 deg; (b) 5 deg; (c) 10 deg; and (d) 15 deg

In Figure 5, the AF target is imaged at unity magnification using a 500-mm-focal-length lens. The Holochip fluidic lens is compared to a Newport KBX-082 lens at each of the four field angles. In Figure 6, the AF target is imaged at unity magnification using a 250-mm-focal-length lens. Again, the Holochip fluidic lens is compared to a Newport KBX-079 lens (FL = 250 mm) at each field angle.

It may be seen that, at both 250-mm and 500-mm focal lengths, and at field angles of 0 and 5 degrees, the Newport lens has slightly better resolution than the Holochip lens (see Figure 5(a,b) and Figure 6 (a,b)). However, at field angles of 10 and 15 degrees, the Holochip lens outperforms the Newport lens at both focal lengths (see Figure 5(c,d) and Figure 6 (c,d)). The loss of quality at field angles of 0-5 degrees is assumed to be caused by slight asphericity in the glass membranes of the Holochip lens. Likewise, the superior performance of the Holochip lens at field angles of 10 and 15 degrees, may also be due to slight asphericity in the membranes.

Modulation transfer function

To corroborate the results of the 1951 Air Force resolution target images, the MTF of four Holochip fluidic lenses and the Newport KBX-082 lens were characterized at a focal length of 500 mm, field angle of 0 degrees and 10-mm aperture. Point spread function (PSF) images were obtained by spatially filtering and collimating the output of a 635-nm laser diode, and focusing the collimated beam with the DUT onto the Sony XC-ST50 camera. Neutral density filters were placed upstream of the DUT in order to reduce the intensity of the focal point being imaged. The captured PSF images were analyzed in MATLAB to create the MTF curves (Figure 7).

The maximum resolvable frequency for all lenses was approximately 10 line pairs per millimeter (lp/mm). The repeatability of these results with all sampled lenses suggests a high degree of confidence in this resolution.

Additionally, the results from the MTF measurements are well matched with the 1951 Air Force resolution target images also measured for each lens (see Figure 5 and Figure 6).

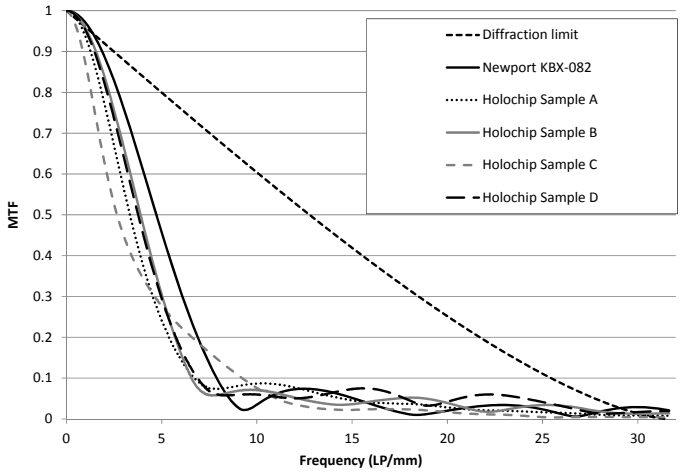

Figure 7. MTF curves for a Newport KBX-082 and four Holochip fluidic lenses set at 500-mm focal length and 10-mm-aperture

The presence of a collimating lens as well as the pixelated image sensor of the camera cause the system MTF to be lower than that of the DUT alone. To correct this, the MTF of a glass lens was modeled in ZEMAX and then the optical assembly tailored to achieve the same results. By varying the strength of the neutral density filters in the system the calculated MTF of the system was matched to that calculated in ZEMAX. With the proper filtering set, the glass lens in the system was replaced with a Holochip lens and the MTF recalculated. To ensure the focal length of the Holochip lens was the same as the Newport lens, the program voltage was adjusted until the spot size detected by the camera was minimized. Figure 7 shows that the MTF curves for the four Holochip lenses and Newport precision glass lens are very similar to each other over the majority of spatial frequencies. Additionally, inspection of the resolution target images in Figure 5 shows blurring substantially similar to that suggested by the MTF curves. This also suggests high confidence in the MTF results.

Life Testing

To assess the effect of extended use on the relationship between program voltage and. focal length, the fluidic lenses were subjected to life testing. The lenses were placed in a collimated HeNe laser beam and the actuator voltage set to midrange (i.e., a program voltage of approximately 2.5 VDC). A pinhole was placed at the focus of the fluidic lens, such that at that particular focal length nearly all of the light passed through the pinhole. Any variation in focal length would thus reduce the light passing through the pinhole. On the side of the pinhole opposite the fluidic lens, a photodetector was placed in line with the beam. The lens was attached to a function generator, varying the program voltage from 0 to 5 VDC. The output of the photodetector was attached to an oscilloscope, thereby displaying a signal proportional to the optical power delivered to the detector as a function of program voltage. The experimental set-up is shown in Figure 8.

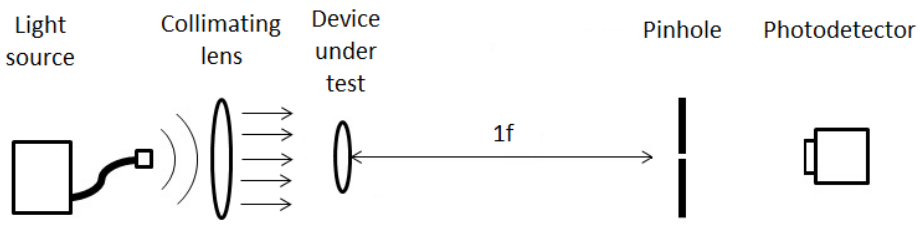

Figure 8. Experimental set-up for life testing fluidic lenses

As predicted, the output from the photodetector closely matched the program voltage signal for the lens. The minimum and maximum values from the photodetector were measured and recorded. Lenses were driven at a frequency of 3 Hz continuously for nearly four days resulting in approximately one million use cycles. During this period there was nominal change in the minimum and maximum recorded photodetector signals. Additionally, both the minimum and maximum focal lengths of the lens were recorded before and after life testing, resulting in no detected change within the error of the measurement. These results suggest little to no change in performance over the one million cycles.

Dynamic response

The response time of the fluidic lens systems was analyzed, again using the set-up shown in Figure 8. In Figure 9 the refractive power as a function of time is depicted for a program voltage step of 5 VDC to 0 VDC and vice versa. The response time of the lens to rise from 0 to 90% of the maximum refractive power is approximately 16 ms. The response time of the lens to fall from 90% to 10% of the maximum refractive power is approximately 12 ms.

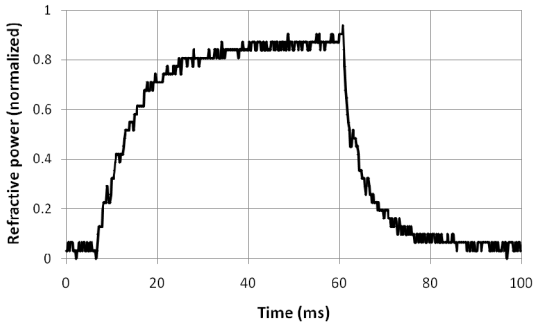

Figure 9. Dynamic response of the fluidic lens

4. CONCLUSION

The design of the 10-mm-aperature fluidic lens comprises dual glass membranes supported by elastomeric seals and aluminum plates. The seals allow the membranes to bend and pivot, achieving an approximately spherical curvature. Actuation is provided by a stack of piezoelectric ring benders integrated into the 25-mm-diamter lens housing. Due to the high stiffness of the glass membranes, the dioptric range is limited to approximately 4 diopters and the focal length ranges from 200 to 900 mm. However, as a trade-off to limited dioptric range, the optical performance of the glass-membrane based fluidic lens is comparable to that of commercial solid glass precision lenses of similar f/# and format. At field angles of approximately 10 degrees or greater, the fluidic lenses outperform the solid glass lenses in terms of resolution. The response time for a fluidic lens with a glass membrane thickness of 70 μm is approximately 16 ms. Lenses were life tested for over 1 million cycles without noticeable degradation in performance. In future work, we will concentrate on methods for improving the dioptric range without sacrificing image quality, as well as designs that increase size of the aperture while providing a high fill factor.

ACKNOWLEDGEMENT

This material is based upon work supported by the DOD/DARPA SBIR Program under Contract No. W31P4Q-09-C-0372 and the United States Air Force under Contract No. FA8650-11-M-1172.

REFERENCES

[1] Nguyen, N.-T., "Micro-optofluidic lenses a review," BIOMICROFLUIDICS 4, 031501, 15pp (2010).
[2] Draheim, J., Schneider, F., Burger, T., Kamberger, R. and Wallrabe, U., "Single chamber adaptive membrane lens with integrated actuation," International Conference on Optical MEMS & Nanophotonics, 15-16 (2010).
[3] Draheim, J., Schneider, F., Kamberger, R., Mueller, C., Wallrabe, U., "Fabrication of a fluidic membrane lens system," J. Micromech. Microeng. 19, 7pp, 095013 (2009).
[4] Draheim, J., Burger, T., Schneider, F. and Wallrabe, U., "Fluidic zoom lens system using two single chamber adaptive lenses with integrated actuation," MEMS 2011, Cancun, MEXICO, 692-695, January 23-27, (2011).
[5] Yang, H., Huang, J.-K., Lin, Y.-F., Fang Shyu, R., Yeh, M.-S., "Low voltage piezoelectricity actuating variable focus plano-convex liquid lens module fabrication," Design, Test, Integration & Packaging of MEMS/MOEMS, 5pp, Seville, Spain, 5-7 May (2010).
[6] Vallet, M., Berge, B. and Volvelle, L., "Electrowetting of Water and Aqueous Solutions on Poly (ethylene terephthalate) Insulating Films," Polymer (Guildf.) 37(12), 2465–2470 (1996).
[7] Xu, S., Ren, H., Lin, Y.-J., Moharam, M. G. J., Wu, S.-T., and Tabiryan, N., "Adaptive liquid lens actuated by photo-polymer," Vol. 17, No. 20, 6pp, OPTICS EXPRESS 17590, 28 September (2009)
[8] Ren, H., Fan, Y. H., Lin, Y. H., and Wu, S.-T., "Tunable-focus microlens arrays using nanosized polymer-dispersed liquid crystal droplets," Optics Communications 247, 101-106 (2005).
[9] Renders, C. A., Kuiper, S.; Hendriks, B. H. W., "Electrowetting module," US Patent 7,327,524, February 5 (2008).
[10] Batchko, R. and Szilagyi, A., "Fluidic lens with manually-adjustable focus," US Patent 7948683, May 24 (2011).
[11] Batchko, R. and Szilagyi, A., "Fluidic lens with manually-adjustable focus," US Patent 7697214, April 13 (2010).
[12] Batchko, R. and Szilagyi, A., "Fluidic lens with reduced optical aberration," US Patent 8064142, Nov. 22 (2011).
[13] Batchko, R.; Mansell, J.; Szilagyi, A.; and Crabtree, A., "Fluidic optical devices," US Patent 7755840, July 13 (2010).
[14] Batchko, R.; Mansell, J.; Szilagyi, A.; and Crabtree, A., "Fluidic optical devices," US Patent 7706077, April 27 (2010).
[15] Batchko, R.; Mansell, J.; Szilagyi, A.; and Crabtree, A., "Fluidic optical devices," US Patent 7701643, April 20 (2010).
[16] http://www.optotune.com/.
[17] Zhang, D.-Y., Justis, N. and Lo, Y.-H, "Integrated fluidic adaptive zoom lens," Optics Letters, Vol. 29, Issue 24, pp. 2855-2857 (2004).